UNIVERSITÀ DI PARMA
ARCHIVIO DELLA RICERCA

University of Parma Research Repository

Assessment of pre-simulated scenarios as a non-structural measure for flood management in case of levee-breach inundations

This is the peer reviewd version of the followng article:

Original
Assessment of pre-simulated scenarios as a non-structural measure for flood management in case of levee-breach inundations / Dazzi, S.; Vacondio, R.; Mignosa, P.; Aureli, F.. - In: INTERNATIONAL JOURNAL OF DISASTER RISK REDUCTION. - ISSN 2212-4209. - 74:(2022), p. 102926.102926. [10.1016/j.ijdrr.2022.102926]

Availability:
This version is available at: 11381/2921124 since: 2024-10-03T16:00:07Z

Publisher:
Elsevier Ltd

Published
DOI:10.1016/j.ijdrr.2022.102926

Terms of use:

Anyone can freely access the full text of works made available as "Open Access". Works made available

Publisher copyright

note finali coverpage

(Article begins on next page)

02 May 2026

Assessment of pre-simulated scenarios as a non-structural measure for flood management in case of levee-breach inundations

Susanna Dazzi*, Renato Vacondio, Paolo Mignosa, and Francesca Aureli

Department of Engineering and Architecture, University of Parma
Viale Parco Area delle Scienze 181/A, 43124 Parma, Italy
*Author for correspondence (susanna.dazzi@unipr.it)

ABSTRACT

Levee breach inundations can entail large flood losses due to the high concentration of exposed assets in levee-protected floodplains and, sometimes, to the inadequacy or absence of early warning systems for this type of events. Since real-time modelling is computationally expensive and presents several uncertainties, which might prevent obtaining a reasonably accurate forecast of the flood propagation, an alternative methodology for the prompt prediction of flooded area, maximum depths, and arrival times during a real event was proposed. The strategy is based on the use of a database of pre-simulated scenarios of levee-breach inundations, obtained adopting a high-resolution two-dimensional shallow water model. The paper aims at the *a posteriori* assessment of the usefulness of this strategy. To this end, the December 2020 event on the Panaro River (Italy) is thoroughly analyzed. In the study area, the strategy had already been implemented before the event, and pre-simulated scenarios were consulted during the emergency. Post-event observations are also available for the ex-post model validation. The database was obtained considering two inflow synthetic hydrographs and a discrete number of breach locations, and unavoidable differences between real events and hypothetical scenarios were to be expected. However, for this case study, the closest levee-breach scenario in the database (in terms of breach position and inflow) provided reliable predictions of flood extent and maximum depths for the actual inundation. The pre-simulated database also helped identifying some critical spots, where effective emergency operations (sandbagging) helped protecting an urban district during the event. As

accurate real-time forecasts of levee-breach inundations are yet to come, a database of pre-simulated scenarios is proven as an effective “surrogate” method for civil protection purposes.

KEYWORDS

Flood scenarios; levee breach; 2D hydraulic modelling; non-structural measures; civil protection activities; inundation forecast

1. INTRODUCTION

Huge economic damage and casualties can occur in flood-prone areas in case of severe flood events (e.g. Salvati et al., 2010; Jongman, 2018). However, the negative consequences of these natural disasters can be mitigated by implementing flood risk management strategies (Plate, 2002), including structural and non-structural measures. Focusing on river floods, the protection of lowland areas from inundation is often guaranteed by the presence of levees, which were progressively heightened and reinforced over the centuries. Hence, the settlement of communities and the concentration of economic assets in these areas kept growing as a result of the sense of security provided by the structural protection system (Ludy & Kondolf, 2012), which can also reduce the preparedness to face adverse flood events (the so-called “levee effect”, see Di Baldassarre et al., 2018). This increase in exposure and vulnerability may lead to catastrophic consequences in case of levee collapse. For this reason, the evaluation of the residual risk associated to levee-breach inundations should be considered in flood management and emergency planning (Tarrant et al., 2005), and numerical modelling can support the flood hazard analyses (e.g. Huthoff et al., 2015; Zhang et al., 2016; Arrighi et al., 2019).

In particular, early warning systems are recognized as effective tools for reducing damage to people and movable assets in case of floods (e.g., Pappenberger et al., 2015; Rai et al., 2020). To issue flood alerts, however, real-time forecasting systems (e.g., Krzhizhanovskaya et al., 2011; Dottori et al., 2017; Ming et al., 2020; Mourato et al., 2021) based on precipitation measurements and/or weather forecasts are required. A number of studies addressed forecasting of river

discharges and water levels at the catchment scale, based on rainfall-runoff modelling (e.g. Masseroni et al., 2017) or machine-learning methods (see the review by Mosavi et al., 2018). Moreover, flood maps and the corresponding impacts (Merz et al., 2020) are increasingly considered in integrated forecasting systems, sometimes thanks to pre-calculated scenarios (e.g., Dottori et al., 2017; Bihan et al., 2017; Bhola et al., 2018; Ritter et al., 2020). In some works, the system can account for potential failures in structural defenses by means of fragility curves (e.g., Bachmann et al., 2016), which provide an estimate of the probability of breach triggering during the event; the consequent inundation is then usually predicted using two-dimensional (2D) hydrodynamic models at coarse resolution (Bachmann et al., 2016) or simplified methods (Kron et al., 2010; Krzhizhanovskaya et al., 2011). Although different failure mechanisms (overtopping, piping, instability) can be considered (Vorogushyn et al., 2010), only few river sections are usually checked for levee failure (Kron et al., 2010; Bachmann et al., 2016), while large uncertainties due to the heterogeneity of earthen materials remain (Oliver et al., 2018). Local weaknesses can be unknown, thus jeopardizing the system's capability of predicting breach triggering and possibly leading to missed alarms. In fact, recent events (Vacondio et al., 2016) indicate that breaches may occur unexpectedly even when the water levels are well below the levee crown elevation, due to local weaknesses in the levee body induced by various causes (plant roots, animal dens, etc.). Moreover, in small-medium river basins with time of concentration of a few hours, a drawback of forecasting systems is the fact that real-time inundation modelling is often challenging due to the required simulation time (Bihan et al., 2017), which is a non-negligible percentage of the physical time, even for computationally efficient 2D hydrodynamic models.

In this framework, Ferrari et al. (2020) recently proposed a new approach with the aim of providing an effective tool to improve preparedness in case of levee-breach inundations in lowland areas. The key idea is to create a wide database of hypothetical plausible flooding scenarios (corresponding to different hydrological conditions and several failure locations along the levee facing the area at risk), which must be simulated using a high-resolution 2D shallow water model. This analysis can be exploited for civil protection purposes, for both planning and carrying out emergency operations in case of an actual levee collapse. In particular, a real event can be related

to the closest simulated hypothetical scenario, so that a comparable “plausible” flood evolution is immediately available to public authorities for the early warning of affected populations, for the organization of evacuations, and for other flood management activities. This strategy overcomes the difficulties of real-time inundation modelling for small-medium river basins, i.e. the long computational times and the necessity of coupling with weather forecasts and/or rainfall-runoff modelling.

This work aims at performing an ex-post assessment of the usefulness of this strategy (i.e., an off-line database of inundation scenarios) for emergency management during a real event. To the best of the authors’ knowledge, other proposed strategies for near-real-time management of levee-breach inundations were only validated by considering hypothetical events or historical events (i.e., occurred when the strategy had not been implemented yet). Conversely, in this paper, the methodology is validated by analyzing a case study for which maps of pre-simulated scenarios were available before the event, and these maps were consulted in the immediate aftermath of the levee failure to support civil protection activities. In particular, the recent event on the Panaro River, where a levee collapse occurred in December 2020 (Menduni et al., 2021) causing an extensive inundation, is considered. Indeed, in this area, a database of hypothetical events was developed just a few months before the event. This makes it an ideal case study to verify the benefits of the pre-simulated scenarios for emergency management purposes. In this work, an ex-post numerical simulation of the real event was first performed and validated with field data to assess the adequacy of the available hydraulic model. Then, the predicted inundation was compared with the results of the closest pre-simulated scenario, which was actually used for flood management during the event. The objective is to evaluate how accurately the flood dynamics could be forecast by taking advantage of the hypothetical scenarios and how this prediction was helpful for emergency activities. As a collateral purpose of this work, the influence of some modelling assumptions (e.g., breach characteristics and location, inflow discharge) on the inundation maps can be investigated by comparing results of the pre-simulated scenario and of the ex-post simulation of the real event.

The paper is structured as follows. In Section 2, the study area is presented and the modelling assumptions for the hypothetical scenarios are listed; moreover, the December 2020 event and the setup for its ex-post simulation are described. In Section 3, the comparison between the results of the simulation of the real event and the post-event observations is first reported; then, the closest hypothetical scenario is identified; finally, a comparison between the numerical results concerning the real event and the pre-simulated scenario is performed as regards flood extent, maximum depths and arrival times. Section 4 discusses the benefits of consulting pre-simulated scenarios during actual inundations and provides guidelines for the application of the strategy in other areas, while the last Section draws the conclusions.

2. MATERIALS AND METHODS

2.1 Study area

Although a database of pre-simulated scenarios can be created for any leveed river, it was originally developed for rivers in the Po Plain (Northern Italy, Figure 1a). Indeed, the overall length of the embankment system along the Po River and its tributaries is more than 2000 km, and several historical breach occurrences are documented in this area (Govi & Maraga, 2005). Levees protect lowland areas characterized by a high concentration of urban settlements and industrial and agricultural activities, but for most tributaries they are not adequate to withstand flood events with medium or low frequency (100-500 years), thus entailing a significant residual flood risk.

Recently, levee failures occurred mainly in the Emilia-Romagna Region, i.e. on the Secchia River in 2014 (Vacondio et al., 2016), on the Enza River in 2017 (Dazzi et al., 2019), and on the Reno, Montone, and Idice Rivers in 2019 (the positions are reported in Figure 1b). The downstream stretch of these rivers is confined on both sides by earthen levees with crest elevations several meters higher than the surrounding lands' level; hence, levee collapses induced extensive inundations. These events raised awareness of the importance of implementing effective strategies to face the residual flood risk and of increasing preparedness in both population and public authorities. To this end, the development of an off-line database of pre-simulated levee-breach flooding scenarios on these rivers is ongoing (Ferrari et al. 2020).

This work focuses on one of the right tributaries of the Po River, namely the Panaro River (total watershed 1780 km^2, upstream watershed 1040 km^2, time of concentration 12-15 h), represented in Figures 1a-1b. In the past, a few levee breaches occurred along its downstream stretch (1966, 1972, 1973, and 1982), while an incipient levee failure was promptly repaired in 2014 (Orlandini et al., 2015), thus avoiding inundations. One of the areas that was hit the most in 1966 and 1973 and that is still threatened by potential levee failures on the right bank of the Panaro River is the Municipality of Nonantola (Province of Modena; ~16'000 inhabitants; ~55 km^2). In light of this, the Municipality commissioned a hydraulic study to the University of Parma, with the aim of updating its civil protection plan. The study, completed in June 2020, included the simulation of ten hypothetical inundation scenarios due to levee breaches in the area (Section 2.2). Unfortunately, only a few months later (December 2020), an actual collapse occurred on the right bank of the Panaro River (Section 2.3), largely affecting the territory of Nonantola.

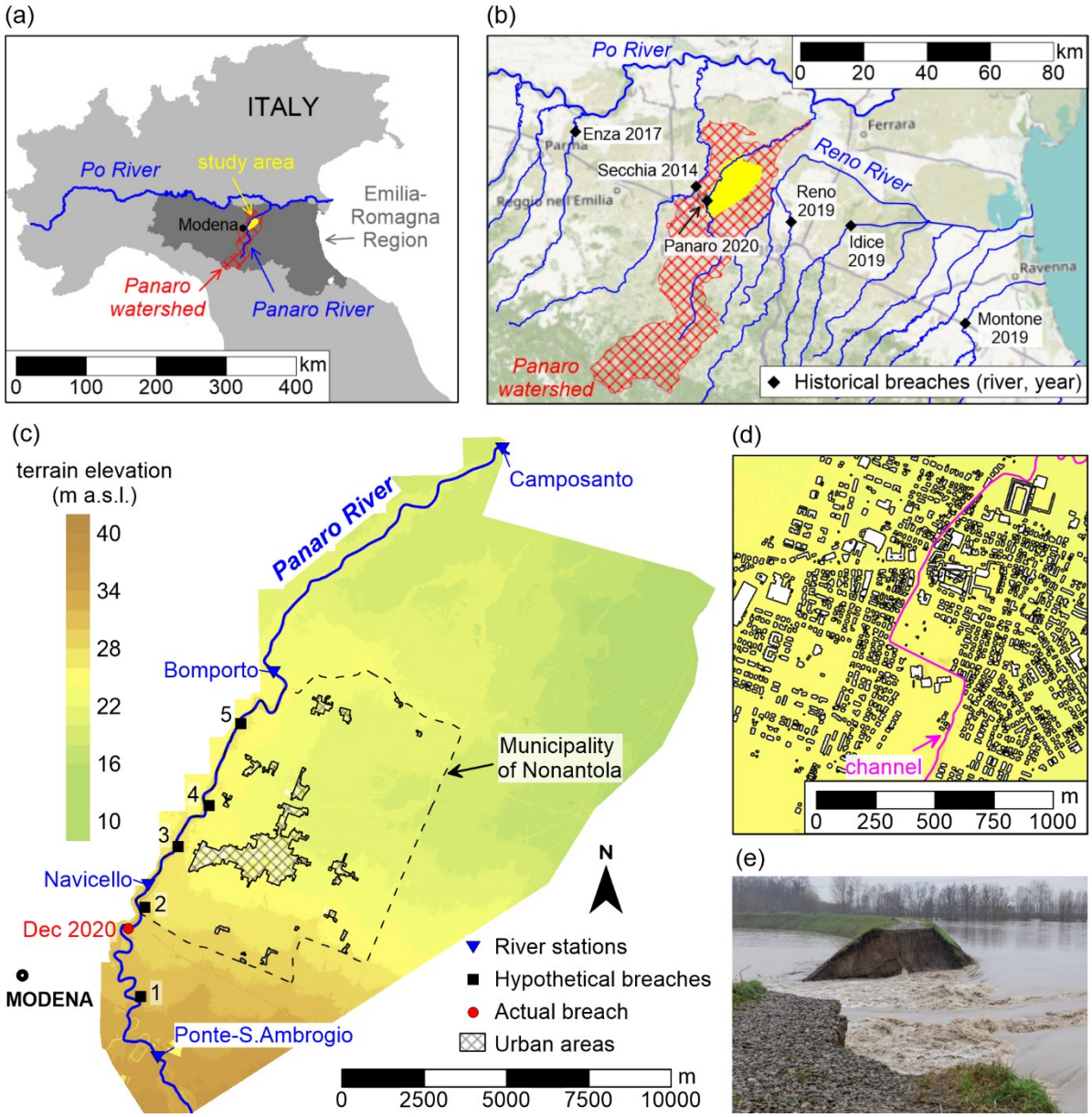

Figure 1. (a) Position of the study area and of the whole watershed of the Panaro River in Northern Italy. (b) Location of six recent breaches (labelled with River name and year) in Emilia-Romagna Region, including the 2020 event on the Panaro River. The blue lines indicate the main rivers in the area. (c) Study area: DTM, river stations, hypothetical and actual breach locations. Only the urban areas in the Municipality of Nonantola are identified. (d) Detail of the town center of Nonantola: the buildings' footprints are identified by black lines, and the Torbido channel is represented in magenta. (e) Breach occurred in December 2020 (photo by Paolo Mignosa).

2.2 Development of the database of pre-simulated inundation scenarios

In this work, the area of interest (Figure 1c) is limited to the 30 km-long stretch of the Panaro River between the gauging stations of Ponte Sant'Ambrogio and Camposanto. The domain also includes the floodable area on the river's right bank (roughly 300 km^2), where the territory of Nonantola is located. The setup for the simulations of hypothetical inundation scenarios in the study area followed the guidelines outlined by Ferrari et al. (2020) and is briefly described in this Section.

2.2.1 Numerical model

The PARFLOOD code (Vacondio et al., 2014, 2017), a 2D model that solves the fully dynamic Shallow Water Equations (SWE) with the finite volume method, was used here. The numerical scheme implemented in PARFLOOD has shock-capturing properties and guarantees a robust treatment of wet/dry fronts and transcritical flows, even for flows over complex topographies. Moreover, the code exploits the computational power of Graphics Processing Units (GPU) to reduce the computational time dramatically compared to serial codes (Vacondio et al., 2014). The model's accuracy and efficiency have been extensively tested for challenging case studies, including levee-breach inundations, in previous papers (e.g. Vacondio et al., 2014, 2016, 2017; Dazzi et al., 2019, 2021), to which the reader is referred for further details. In this work, all simulations were run on a NVIDIA V100 GPU.

2.2.2 Topographic data and spatial resolution

The area is fully covered by a 1 m-resolution Digital Terrain Model (DTM) obtained from Lidar surveys, which was down-sampled to 2 m-resolution. A Block-Uniform Quadtree (BUQ) grid (Vacondio et al., 2017) was used for computations, and the highest resolution (2 m) was imposed along the river (channel and levees), along the main road embankments and levees of minor channels, and in urban areas, while a lower resolution (up to 16 m) was used for rural areas. Buildings (see Figure 1d) were explicitly resolved in the computational mesh and treated according to the "Building Hole" strategy (Schubert & Sanders, 2012). Overall, the domain was discretized with 14 million cells.

2.2.3 Roughness

The river calibration was performed by simulating three past flood events (without breach) with different roughness coefficients until the configuration that best matched the recordings at the gauging stations of Navicello and Bomporto was identified.

As regards the floodable area, past inundation events were rather old (1966, 1973) and could not be used for calibration due to the unavailability of quantitative reliable field data and to the great modifications occurred in the area since then (river engineering works; urban expansion and change in land use; building of new infrastructure, e.g. high-speed railway, bypass road, etc.). If a closer-in-time inundation had occurred in the area, field data collected from that event would have been valuable for the roughness calibration, but this was not the case when the database was created (the real event occurred months later). Therefore, the results of the calibration performed by Vacondio et al. (2016) for an inundation that occurred on a nearby area with similar land use were exploited here; accordingly, Manning's roughness coefficient was assumed equal to 0.05 $m^{-1/3}s$ for the whole floodable region (mainly rural).

2.2.4 Hydrological conditions

Two Synthetic Design Hydrographs (SDHs) with different return periods were considered as hydrological inputs for the present analysis. SDHs were obtained from the statistical analysis of the series of historical floods at Bomporto station, following the procedure described by Tomirotti & Mignosa (2017). As discussed by Ferrari et al. (2020), at least two different hydrological conditions should be considered when creating the database, namely an event potentially responsible for overtopping-induced breaches ("Inflow A") and a less severe event that still has the potential to trigger breaches due to piping or other collapse mechanisms ("Inflow B"). For this study area, the event with a return period of 200 years, which generates water levels that exceed the levee crest elevation along the Panaro River, was assumed for "Inflow A" scenarios, while a higher probability event (1/20 years) was considered for "Inflow B" scenarios. Moreover, the 200-years hydrograph is also the reference event for flood hazard assessments in regional planning, according to the Italian regulations. It is worth clarifying that the estimation of the probability of breach collapse during these events is outside the scope of this work.

213 ***2.2.5 Levee breach locations and modelling***

214 Five hypothetical breach locations (labelled 1-5 in Figure 1c) on the right levee of the Panaro River,
215 with 2-3 km spacing, were considered. The breach opening was simulated using a “geometric”
216 approach: the breach depth and width evolve linearly from zero to the prescribed final geometry in
217 a pre-defined opening time (Ferrari et al., 2020). For both hydrological scenarios, a final breach
218 width equal to 100 m was adopted, whereas the opening time was assumed equal to 3 h and 6 h
219 for Inflows A and B, respectively. These assumptions were based on historical experience of past
220 breaches occurred on similar rivers in the same region (Vacondio et al., 2016; Dazzi et al., 2019).

221 ***2.2.6 Other assumptions and outputs***

222 A stage-discharge relationship at Camposanto (14 km downstream from the last breach location)
223 was assumed as outflow boundary condition on the river. Simulations were prolonged for 48 h after
224 the breach triggering: it is very likely that, after this timespan, the flood propagation would be
225 significantly affected by emergency operations, which were not considered when simulating these
226 scenarios.

227 As outputs, animations of the flood evolution and maps of maximum water depths, maximum flow
228 velocities, and arrival times were provided for each of the 10 simulated scenarios in the database
229 (2 inflows × 5 breach positions).

230 Finally, it is worth clarifying that the number of pre-simulated scenarios, in terms of spacing of
231 breach locations and inflow conditions, was selected as a good compromise between the
232 achievement of a “manageable” database (storage, accessibility, ease of consultation) and the
233 necessity of providing reliable predictions for possible future real events, which must cover different
234 possible inundation patterns. This issue will be discussed in more detail in Section 4.2.

235

236 **2.3 Description of the real event**

237 The Panaro River experienced a levee breach on the right bank (Figure 1e) on 6th December 2020
238 during a medium-severe flood event, which was induced by the persistent heavy rainfalls on the
239 Panaro watershed on 4th-6th December 2020 and aggravated by the concurrent melting of snow.
240 The breach was triggered around 6:00 a.m. in the location shown in Figure 1c. The river water

stages were well below the levee crest elevation; hence, the breach was not induced by overtopping. Post-event surveys (Menduni et al., 2021) revealed that the levee material was locally heterogeneous, with the likely presence of dead stumps of an invasive plant species (*Arundo Donax*); possibly, preferential flow pathways triggered back erosion through the levee body, leading to the levee collapse; moreover, the seepage may have been exacerbated by the possible presence of cavities due to burrowing animals (observed at nearby sites, see Orlandini et al., 2015). The breach reached a final width of almost 80 m after a few hours, and the levee was fully repaired after almost one day (provisional closure operations ended on 7th December at 8:30 p.m.). The estimated flooded area was around 14 km^2, most of which belong to the territory of Nonantola. The inundation caused heavy consequences, including people displacement, service disruption, and huge economic damage to the residential and productive sectors. As an indication, the estimated damage was reported to be around 50M€ just for residential properties (Manselli et al., 2022) and 5M€ just for public properties.

2.4 Setup for the ex-post simulation of the real event and available data

The ex-post 2D simulation of this event was performed with the same numerical code (PARFLOOD) and adopting the same modelling assumptions of the pre-simulated scenarios as regards topography and roughness. The simulation starts on 5th December at 0:00 a.m. and ends on 7th December at 6:00 p.m. (66 h of physical time). The stage hydrograph recorded at Camposanto was imposed as downstream boundary condition, while the inflow discharge was obtained from the recorded water stages at Ponte Sant'Ambrogio. Since the presence of the breach can affect the upstream water levels due to the formation of a drawdown profile, two different rating curves (before and after the breach opening) were adopted to convert the water levels into discharge values, as suggested in previous works (Vacondio et al., 2016; Dazzi et al., 2019). In particular, the two stage-discharge relationships were obtained numerically by simulating the propagation of synthetic hydrographs along the river in two configurations (without the breach, and in the presence of a fully developed breach), following the procedure described in detail by Vacondio et al. (2016).

269 The final breach width was set equal to 80 m according to field observations, while the timing
270 parameters for the breach opening were calibrated in order to reproduce the recorded water levels
271 at the gauging station of Navicello (Figure 1c), located only 1.5 km downstream from the breach
272 location.
273 Soon after the breach opening and the lowland inundation, emergency activities were undertaken
274 to drain the flooded waters at multiple locations, by exploiting the drainage and irrigation channels
275 and by using draining pump stations. Clearly, all these operations were neglected in the simulation.
276 Only one emergency intervention was modelled, i.e. the blockage of two roads with sandbags to
277 prevent water from reaching the Eastern part of the town of Nonantola. In the simulation, the
278 blockage was simply considered by raising the terrain elevation in a few cells across the streets.
279 This intervention will be discussed more in detail in Section 3.1.
280 Some field data were available to validate the ex-post simulation of this event. The Municipality of
281 Nonantola provided an approximate boundary delimitation of the flooded area obtained from a
282 quick terrestrial survey performed on 7th December. Additionally, a few qualitative information and
283 quantitative measures of indoor and outdoor water depths at selected locations were collected
284 after the event. The dataset was divided into two sets of points:

285 • "perimeter" points, which can be used for an independent verification of the approximate
286 boundary of the flooded area in some locations;
287 • points with associated maximum inundation depth (watermarks), mainly located in the
288 urban area.

289 The second set of data was further refined by excluding all points with depth below 15 cm, which
290 were considered too uncertain (comparable to the accuracy of the Lidar survey). Overall, 50
291 watermarks were retained. Depth values were then converted into water surface elevations by
292 adding the local terrain altitude (10 cm were also added for indoor points wherever a doorstep was
293 identifiable). It is worth noting that the collection of post-event data is associated with large
294 uncertainties: the accuracy of watermarks can be up to 50 cm, according to Dottori et al. (2013).
295 For this reason, this dataset was only used to check the overall model performance in predicting
296 the inundation.

3. RESULTS

3.1 Ex-post simulation of the real event vs. field observations

This Section is dedicated to the validation of numerical results for the ex-post simulation of the December 2020 flood event.

The final breach width, set equal to 80 m as reported by the flood management personnel, was not modified during calibration. However, breach-timing parameters influence the prediction of levels at Navicello gauging station and were defined by trial-and-error. A good agreement between numerical results and recorded levels was achieved with the following assumptions: (i) the breach was triggered at 5:30 a.m. on 6th December, and (ii) the vertical and lateral growth rates were about 4 m/h and 10 m/h, respectively. According to this latter assumption, in the simulation the levee crest deepened to the local ground elevation in about 1 h, while the breach widening phase lasted about 8 h. This is consistent with the typical breaching mechanism of earthen dams (e.g., Visser, 1999; Viero et al., 2013). Figure 2a shows that the model reproduces the water levels at Navicello gauging station very well.

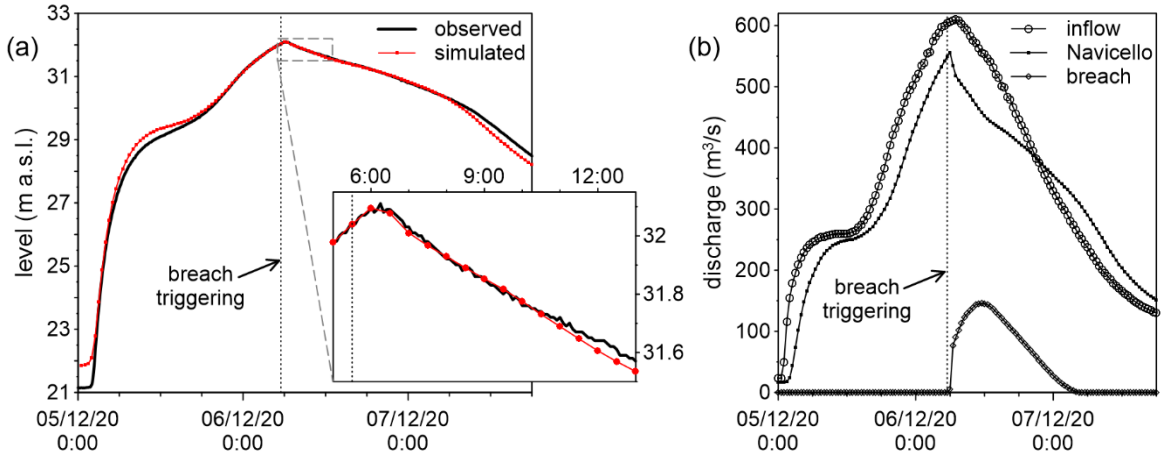

Figure 2. (a) Simulated and observed levels at Navicello gauging station. (b) Simulated discharge hydrographs at Ponte Sant'Ambrogio (inflow), at Navicello, and breach outflow.

The simulation results concerning the breach outflow discharge are reported in Figure 2b, together with the hydrographs at Ponte Sant'Ambrogio (inflow) and at Navicello (downstream of the breach).

318 The breach outflow volume can be estimated around 6 Mm^3, and the peak discharge flowing
319 through the breach is close to 150 m^3/s.
320 Figure 3a reports the approximate delimitation of the actual flooded area (dashed line) that was
321 quickly surveyed after the event, and the locations of additional “perimeter” points, i.e. labelled as
322 either “on the limit of the flooded area” (orange symbols) or as “remained dry” (magenta). Overall,
323 these points confirm the approximate boundary of the actual inundation, being only slightly more
324 accurate on the Eastern limit, where flooding was actually delimited by the left levee of the Torbido
325 channel that crosses the town (see detail in Figure 3b), also thanks to emergency operations.
326 Inside the urban area, the Torbido channel is culverted and a slightly raised cycle path lies on top
327 of it, but the cycle path elevation is locally lowered at two crossroads (maroon symbols in Figure 3).
328 The continuity of this slightly elevated topographical feature is therefore locally interrupted, and
329 pre-simulated flooding scenarios indicated that this could be a critical spot (as will be discussed in
330 Section 3.2.2). However, during the event, sandbags and loose earth were placed at these
331 locations in order to create a provisional flood barrier that successfully protected the Eastern part
332 of the town.
333 The inundation boundary in Figure 3a also shows that other road embankments and minor channel
334 levees influenced the flood propagation, especially in the Northern district, but also close to the
335 breach site.
336 The inundated area obtained from the ex-post simulation is represented in Figure 3a in terms of
337 contour map of maximum water depths. In general, the maximum depths are below 1.5 m, except
338 for accumulation areas or upstream of road embankments that are eventually overtopped. The
339 inundation extent generally agrees with the flooded area reported by the local authorities. The
340 interference of linear terrain features, which generate multiple propagation fronts to the North and
341 confine the inundation to the East, is well captured. The main discrepancy with the actual
342 delimitation can be observed downstream, in the North-Eastern part of the domain. Here, towards
343 the end of the simulation, the model predicts the accumulation of the flooded volume in a rural area
344 bounded by minor channels, and the inundated area is overestimated. However, this error can be

345 mainly ascribed to the lack of a detailed simulation of how the complex drainage system (including
346 gates and pumps) was managed during the event.
347 Figure 3b zooms on the urban area of Nonantola and shows that only very limited flooding (a few
348 centimeters) is predicted in the Eastern part of the town. This was possible thanks to the inclusion
349 of the local terrain raise in the simulation, which mimics sandbagging operations during the event.
350 The location of the 50 surveyed watermarks is also reported. The color-coding of symbols refers to
351 the error of simulated maximum levels compared to observations, and circles and triangles indicate
352 under- and over-prediction, respectively. In most locations (roughly 72%), the simulated depth
353 differs less than 30 cm from the surveyed value. The average error is +4 cm, while the Root Mean
354 Square Error (RMSE) and the Mean Absolute Error (MAE) are equal to 29 cm and 23 cm,
355 respectively. Given the large uncertainties of this kind of surveyed data, which especially affect
356 indoor values, the agreement can be considered quite satisfactory. Besides, in the urban area, the
357 simulation neglects the flooding of basements and sewer systems, which may have contributed to
358 storing a fraction of the flooded volume and to slightly reducing the surface water levels.
359 Finally, reliable information about the flood arrival times was scarce. According to the post-event
360 report (Menduni et al., 2021), the inundation reached the town of Nonantola approximately 6 h after
361 the breach opening (i.e. around 12 a.m.), although precise locations and arrival times are not
362 mentioned. In the simulation, the Southern district of the urban area is flooded between 11:30 and
363 12:30 a.m., which is in agreement with this indication (only slightly anticipated). The whole map of
364 flood arrival times is reported and discussed in Section 3.2.2.
365 Although a specific calibration of the roughness coefficient for the floodable areas was not
366 performed, these results suggest that the assumptions made during the model setup for the pre-
367 simulated scenarios were reasonable for this study area, and, consequently, that this model can
368 predict the inundation due to a levee breach with satisfactory accuracy.

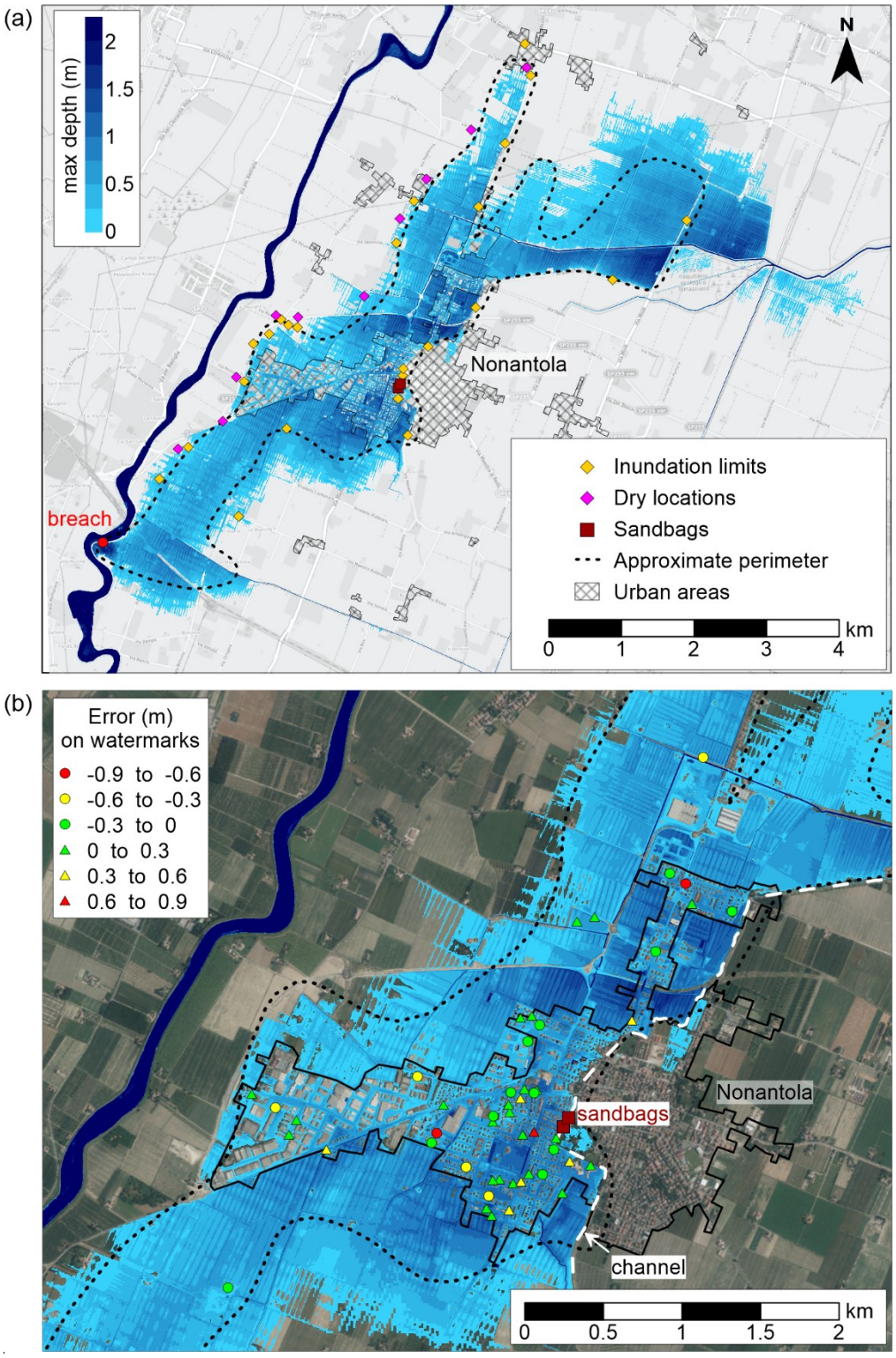

Figure 3. Comparison of simulation and field observations for the event of December 2020. (a) Simulated map of maximum water depths, boundary of the actual flooded area, and "perimeter" points. (b) Detail of the urban area of Nonantola: map of maximum water depths (same color bar as panel a), and color-coded symbols indicating the error of simulated vs. observed water depths at the watermarks' locations.

3.2 Ex-post simulation of the real event vs. closest hypothetical flooding scenario

3.2.1 Identification of the closest scenario

The actual breach occurred in a position that is between the hypothetical breaches 1 (the distance is about 3 km) and 2 (only 800 m downstream), as can be seen in Figure 1c. Therefore, the closest breach scenario from the database was selected as the one following the hypothetical opening of Breach 2.

As for the hydrological conditions in the river, the database of pre-simulated scenarios includes two possible flood events, with return periods T of 20 and 200 years, respectively. In Figure 4, the inflow hydrograph of the real flood event is represented with the SDHs characterized by different return periods. The figure also reports the SDHs with T = 50 and 100 years for comparison and visualization purposes, even if these hydrographs were not considered when creating the database (Section 2.2).

The estimated peak discharge of the 2020 flood is slightly higher than 600 m^3/s, while the hydrograph's volume is around 80 Mm^3. Overall, the event looks close to the 1/50 years' hydrograph (similar peak, slightly lower volume especially in the recession limb). The hydrograph with T = 200 years is characterized by larger peak and volume (around 700 m^3/s and 100 Mm^3, respectively), whereas the one with T = 20 years is closer to the actual event in terms of volume (about 73 Mm^3), even if the peak discharge is lower (530 m^3/s). This analysis suggests that, among the hydrological conditions available in the database, the 1/20 years' scenario is the closest to the actual flood event. It is worth noting that the "Inflow B" type of flood was specifically included in the database as a hypothetical event that may generate breaches due to piping or internal erosion (no overtopping), similar to the December 2020 event. Since the discharge may be unavailable or difficult to be predicted in real time, this consideration could help in the quick selection of the closest inflow scenario ("Inflow A" for breaches induced by overtopping, "Inflow B" for other failure mechanisms), as the occurrence of overtopping is somehow related to the severity of the event.

In summary, the inundation map related to the hypothetical scenario of Breach 2 with "Inflow B" (T = 20 years) was extracted from the database and compared with the ex-post simulation of the actual flood. During the event, this pre-simulated scenario was also consulted by the flood

management personnel. In order to provide an example of how much the correct identification of the closest scenario (breach location, type of inflow) may influence the flood maps to be used for civil protection purposes, Appendix A compares the flooded areas for a few different scenarios, corresponding to Breaches 1, 2, and 3 with T = 20 and 200 years. Although the flooded areas are partially different, the maps show that the urban center of Nonantola would be inundated quite comparably to what happened during the 2020 event.

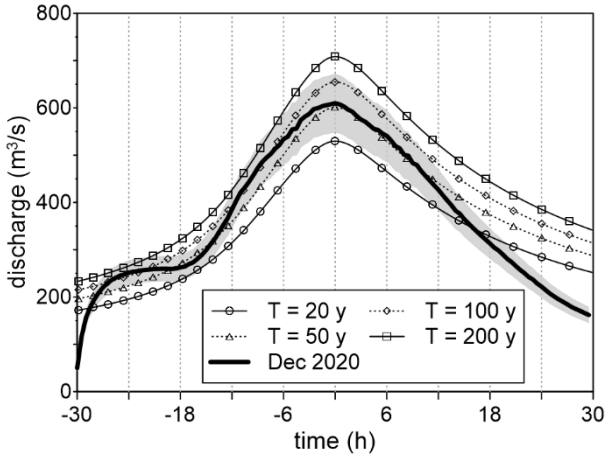

Figure 4. Comparison between the SDHs with different return periods and the estimated inflow for the 2020 flood event in the Panaro River. Dashed lines indicate SDHs not considered in the database of pre-simulated scenarios. The grey band is a rough indicator of the uncertainty in the discharge estimation (±10%) for the real event.

3.2.2 Comparison of numerical results

Table 1 summarizes the main features of the two simulations regarding the real event and the closest pre-simulated scenario (Breach 2, “Inflow B”). Differences concerning the inflow hydrograph in the river, in particular the peak discharge, have already been discussed in Section 3.2.1. Moreover, the two simulations differ in terms of breach modelling. Apart from the different breach location (entailing also a different floodplain width), the *a priori* assumptions for the hypothetical scenario (see Section 2.2) included a wider breach (100 m) and no distinction between vertical and horizontal opening times (both 6 h).

Table 1. Main features for the simulation of the actual event and of the closest hypothetical flooding scenario in the RESILIENCE database (Breach 2, Inflow B).

	Simulation features	Event of December 2020	Hypothetical scenario
Inflow hydrograph	Peak discharge in the river (m^3/s)	610	530
	Hydrograph's volume (Mm^3)	80	73
Breach modelling	Breach location	See Figure 1c	See Figure 1c
	Floodplain width at breach site (m)	40	20
	Breach final width (m)	80	100
	Breach opening time - vertical (h)	1	6
	Breach opening time - horizontal (h)	8	6
	Simulated time after breach triggering (h)	36	48
Simulation results	Flooded area (km^2)	17	23
	Breach outflow volume (Mm^3)	6	14
	Physical/computational time ratio (-)	10.7	7.2

Despite these differences, the flooded areas for the two scenarios are quite similar. The map of maximum water depths for the pre-simulated scenario is reported in Figure 5a and has to be compared with the map obtained for the ex-post simulation of the December 2020 event, shown in Figure 3a. To ease the comparison, Figure 5a also reports the non-fragmentary boundary (red line) of the simulated flooded area in Figure 3a for the real event. Moreover, Figure 5b shows a map of the water level differences between the hypothetical scenario and the ex-post simulation, which confirms their good overlap. Clearly, near the breach sites, the two maps show remarkable differences, but the predicted maximum depths become quite similar moving downstream. The pre-simulated scenario is characterized by slightly higher water depths, which is expectable considering the much larger breach outflow volume (Table 1), but the differences are below 25 cm in most of the domain, especially in the urban area of Nonantola. Further downstream, larger deviations can be observed. In the North-Eastern part of the domain, the hypothetical scenario is slightly more severe than the real flood (larger inundated area and higher levels), in line with the larger breach outflow volume and, possibly, also with the slightly more prolonged simulation. In this area (mostly rural), the numerical model predicts water accumulation, which could actually be relieved by drainage operations during real events.

Another discrepancy is related to the flooding of the Eastern district of the town of Nonantola, which is present only in the hypothetical inundation. As a matter of fact, the results of this scenario

(already available before the real event) led to the identification of the critical spots in the cycle path embankment, and sandbags were therefore placed here during the 2020 event with the aim of hindering the inundation to the East (see Section 3.1). This is reflected in the numerical results of the ex-post simulation, where this emergency intervention was considered. This difference can also be noticed in the values of the flooded areas reported in Table 1.

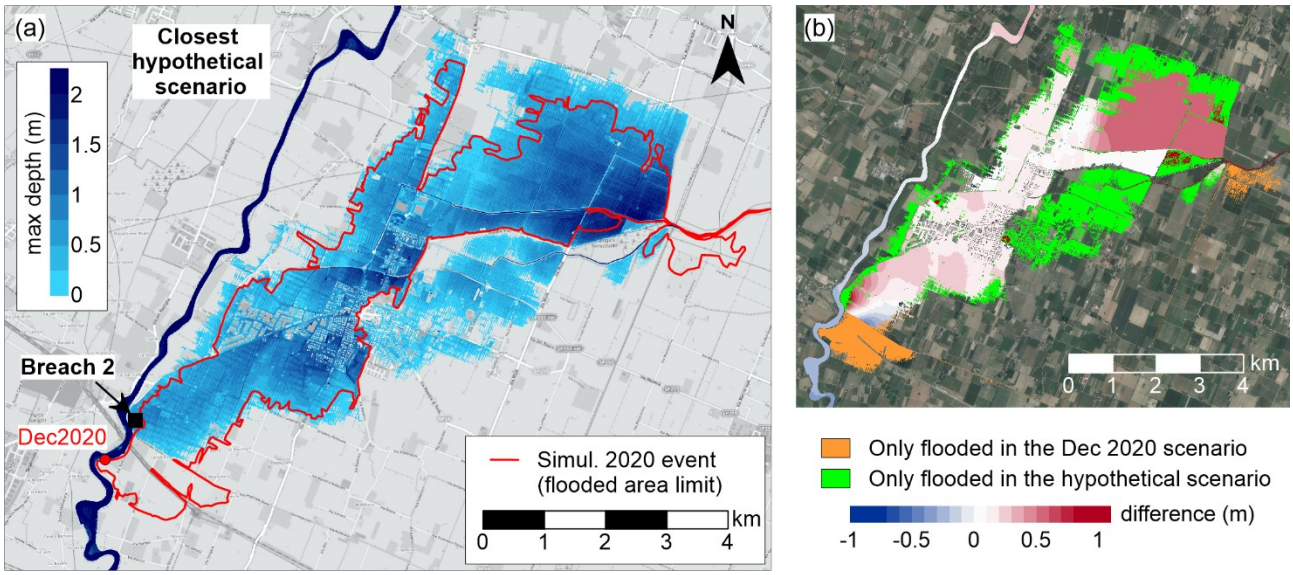

Figure 5. (a) Maximum water depths for the "Breach 2 Inflow B" scenario in the database compared with the non-fragmentary delimitation of the flooded area for the ex-post simulation of the 2020 event (red line). (b) Water level difference between the closest pre-simulated scenario and the ex-post simulation of the event.

The availability of the expected flood arrival time at different locations can be very helpful for emergency management. Figure 6 compares the maps of arrival times obtained from the two simulations (real vs. hypothetical event). Although a thorough validation of this map for the 2020 event could not be performed due to lack of reliable observed data, at least the arrival time in the urban area of Nonantola matched the scarce available information acceptably (see Section 3.1). The comparison with the hypothetical scenario shows that the breach location influences the flood arrival time. The Western part of the town of Nonantola is flooded after 5-9 h from the breach triggering in the real event simulation, while the hypothetical scenario predicted an earlier

inundation (after only 4-8 h). These differences can be mainly ascribed to the closer proximity of the breach site to the town in the latter case compared to the real event, but also, to a lesser extent, to the lack of interferences with road/railway embankments that are capable of delaying the inundation in this part of the territory. Conversely, during the real event, one road and one railway embankment, transverse to the main direction of the inundation and located about 500-800 m downstream of the real breach (but upstream of hypothetical Breach 2, see also Figure 3a), slightly obstructed the flood propagation.

Downstream of Nonantola, similar differences in the arrival times can be observed, i.e. the hypothetical scenario provides shorter arrival times (around 1-2 h earlier, up to 2.5 h further downstream). As an example, to ease the comparison, Figure 6 reports the arrival time at three locations (roughly 3 km apart from each other) in both scenarios. The travel time of flooding from one location to the next also appears a bit shorter in the hypothetical scenario. In fact, due to the slightly higher water levels, the embankments are overtopped or circumvented earlier in this latter simulation compared to the ex-post simulation of the event.

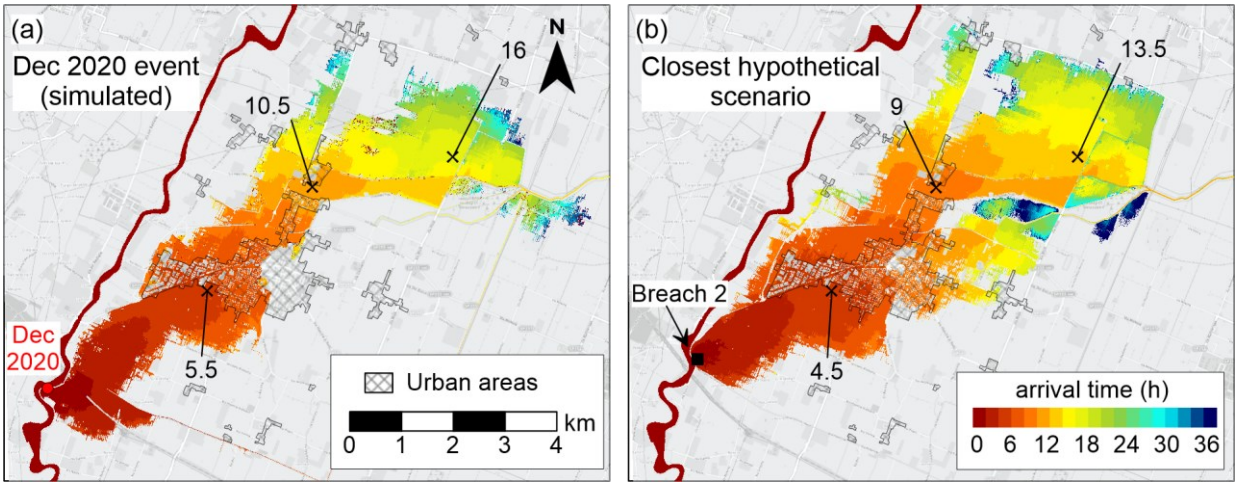

Figure 6. Comparison of the simulated flood arrival time for (a) the December 2020 event, and (b) the closest hypothetical scenario. In both maps, initial time corresponds to the breach triggering. The arrival times at three selected locations (cross symbols) are also reported to ease the comparison.

4. DISCUSSION

4.1 Validation of the methodology

This work aimed at assessing the usefulness of an off-line database of pre-simulated levee-breach scenarios that can be exploited to organize emergency activities in case of a real event, i.e. to predict the inundation dynamics (inundated area, maximum depths, and flood arrival times) and, if possible, to identify countermeasures aimed at reducing the potential damage. To this end, the 2020 event on the Panaro River was considered as case study.

First, it was verified that the 2D hydraulic model previously set up to simulate the hypothetical scenarios could reproduce the real event occurred on the Panaro River in 2020 in an acceptable way, even in the absence of an ad-hoc calibration of roughness coefficients for the floodable area. The assumptions made for another nearby area with similar land use (i.e. the Secchia River levee-breach real case reported by Vacondio et al., 2016) were applied to this case study. Previous works (e.g., Yu & Lane, 2006; Liu et al., 2019; Dazzi et al., 2021) investigated the influence of roughness on the inundation extent by means of sensitivity analyses, showing that these parameters often depend on the adopted model and on the mesh resolution. However, the same model (PARFLOOD) and comparable mesh resolutions (5 m for the Secchia case study, and 2-4-8-16 m here) were used, hence the adoption of the same roughness values was considered suitable when setting up the model. The results of the ex-post simulation of the 2020 event confirmed the adequacy of this assumption. In fact, overall, the adherence of the simulated flooding to observations is satisfactory in terms of inundated area and maximum water depths (see Section 3.1). This assessment confirms *a posteriori* that the database of pre-simulated scenarios can be considered reliable for prediction purposes.

To benefit from the results available in the database, the closest hypothetical scenario was identified, i.e. the scenario with the closest breach position and the hydrological condition most similar to the real event in the river. Obviously, the hypothetical and real events show some differences in terms of inflow flood hydrograph and of assumptions on breach characteristics and development (position, width, opening time), as described in Section 3.2.1. Despite these differences, the predicted flooded area and maximum water depths that could be inferred thanks to

514 the simulation of the hypothetical scenario are overall in fairly good agreement with the real event,
515 except for some expectable discrepancies near the breach site (see results in Section 3.2.2).
516 Moreover, the comparison between results of hypothetical and ex-post scenarios sheds some light
517 on the influence of breach parameters on the flooding. Recently, Tadesse & Fröhle (2020)
518 investigated the sensitivity of inundation to several breach parameters, and concluded that the
519 most influential factors were the breach dimensions and location. However, the present study
520 shows that, as long as the distance between two breach locations is adequate, the different breach
521 position does not represent an issue for obtaining a sensible flood map (except very close to the
522 breach site). Additionally, Ferrari et al. (2020) performed a sensitivity analysis on a breach
523 inundation, showing that the flooded area is only marginally influenced by the breach development
524 time and final width (as long as these are consistent with the river characteristics), and that
525 differences in the inflow hydrographs may not be critical for predicting the flooded area. In fact, in
526 lowland areas, the inundation is often limited by topography and linear terrain features, hence the
527 maximum depths increase when the breach outflow volume is larger, while the flooded area extent
528 might be less influenced. These observations are confirmed by the present study, where the
529 largest differences in the flooded area are actually due to the lack of inclusion of sandbagging
530 operations in the hypothetical scenario (see Section 3.2.2), and not to the different breach outflow
531 volume. This discussion suggests that the results from the database can be effectively exploited for
532 predicting the inundation extent expeditiously during emergencies, even if the pre-simulated
533 scenarios do not exactly match the current conditions.
534 On the other hand, the flood arrival times obtained from the hypothetical scenario present
535 somewhat large differences from the ex-post simulation of the real event, due to the fact that the
536 hypothetical breach position is closer to the vulnerable areas, leading to earlier flooding. The
537 magnitude of the breach outflow volume also influences the travel time. Therefore, predictions
538 regarding the flood arrival times should be used carefully, and an uncertainty at least in the order of
539 1-3 h should be taken into consideration. Nevertheless, at locations that are expected to be
540 inundated at least a few hours after the breach opening, the rough indication of the flood arrival
541 time can still be useful for alerting the population and, possibly, for moving vehicles or other assets.

542 This actually occurred during the flood event herein analyzed. Moreover, maps of depths and
543 arrival times can be used for evacuation planning (e.g., Zhang et al., 2016) in the areas at highest
544 risk.
545 Besides early warning, knowing the flooded area in advance can also be helpful for practical
546 emergency activities. This case study provided an example of how the maps from the database of
547 pre-simulated scenarios were used to optimize the use of sandbags and other temporary barriers
548 that proved effective to reduce the total flooded area. In particular, the hypothetical scenario
549 suggested that two critical spots were responsible for the partial flooding of the Eastern part of the
550 town of Nonantola, though with low depths. This inundation was avoided during the real event
551 thanks to prompt sandbagging. This emergency operation is clearly case-dependent, but effective
552 strategies can be devised on a case-by-case basis and may include flood barriers, relief cuts,
553 pumping, etc.
554 One may argue that a real-time simulation (e.g. Kron et al., 2010; Nguyen et al., 2015; Bachmann
555 et al., 2016) could have been performed instead of using the results from the database of pre-
556 simulated scenarios, given that the 2D hydraulic model for the study area was already available.
557 However, several issues prevented this in the practice, the most important being the unavailability
558 of a reliable upstream boundary condition for running the simulation up to many hours after the
559 breach triggering. Indeed, the inflow discharges that could be obtained from a rainfall/runoff model
560 of the upstream watershed would be characterized by large uncertainty and partly depend on
561 weather forecasts, given the relatively short time of concentration of the watershed (e.g. 12-15 h
562 for this case study). Moreover, the available model was not setup in an “optimized” way for real-
563 time simulations. In particular, the model (grid resolution of 2 m, building representation) is too
564 detailed for achieving quick results, but the cost of long computational times (in the order of 2-6 h,
565 see physical to computational time ratios reported in Table 1) is counterbalanced by a very
566 accurate representation of the study area. For near-real-time simulations, a model with a slightly
567 coarser mesh size (5-10 m) and a more simplified building treatment (e.g. increased roughness in
568 urban areas) should have been preferred, as it would still be adequate for a rapid inundation
569 assessment and would require much shorter runtimes (<1 h). Finally, the implementation of a real-

570 time flood prediction system requires a dedicated computational platform, trained personnel, etc.,
571 tools and skills that are rarely available, complex to organize and expensive to maintain for minor
572 rivers. Conversely, the database of pre-simulated inundations can be easily accessed after the
573 actual breach triggering, the identification of the closest scenario is quite straightforward as regards
574 the breach position and the inflow conditions (see Section 3.2.1), and the maps of results can be
575 quickly uploaded in GIS environment to identify areas at risk and organize emergency operations.
576 Finally, it is worth stressing that, among the available approaches in the literature for the near-real-
577 time prediction of levee-breach inundations, the methodology based on pre-simulated scenarios is
578 the first one whose effectiveness could be validated *a posteriori* in this work, thanks to its
579 implementation in the study area prior to the actual event.
580

581 ## 4.2 Application to other areas

582 Based on the experience gained from this event, some guidelines for the application extension of
583 the proposed methodology to other areas are here briefly discussed to supplement the indications
584 already provided by Ferrari et al. (2020).
585 In general, pre-simulated scenarios can be useful in any lowland area protected by river levees.
586 The only limitation for a practical implementation concerns the availability of recent and accurate
587 terrain data (e.g. DTMs from high-resolution LiDAR surveys). Indeed, lowland inundations are
588 mainly driven by topography and, therefore, the accuracy of scenarios is subject to the correct
589 representation of terrain features, which is guaranteed by the adoption of high-resolution grids.
590 Simulating large domains using fine grids, however, requires an efficient 2D hydrodynamic model
591 in order to achieve affordable runtimes. Parallel codes are therefore recommended, and fully
592 dynamic SWE models with shock-capturing properties should be the preferred choice in order to
593 avoid the possible loss of accuracy entailed by simplified models and the numerical instabilities
594 that may arise in case of transcritical flows. These modelling choices guarantee that the
595 uncertainties related to topography and physical representation of the phenomenon are
596 substantially reduced.

On the other hand, a somehow larger uncertainty remains as regards the roughness of the floodable area. Calibration can only be performed if inundations have recently occurred in the area, which is often not the case. Useful indications can sometimes be obtained from events in nearby areas with similar land use, if available (similar to the present work), but in all cases a reasonable range of roughness values can at least be inferred from the literature based on the land-use type. In fact, previous works (Dazzi et al., 2021) show that, if roughness coefficients are assumed sensibly, their choice does not affect the inundated area and maximum water levels significantly for topography-driven inundations, as long as a high-resolution grid and a fully dynamic 2D-SWE model are used. Conversely, the influence of roughness is more evident on the flood arrival times. For example (Dazzi et al., 2021), the uncertainty on this result can be in the order of 1 h for locations that are flooded within 10 h, and up to 2-3 h for locations that are flooded after 24 h from the breach triggering. Results from the present work, however, highlight that a similar uncertainty in flood arrival times can derive from other sources, such as differences in the breach location and in the breach outflow volume. For this reason, while on the one hand the large uncertainty in the flood arrival times is recognized as a possible limitation of the proposed methodology, on the other hand it puts the issue of roughness calibration in perspective.

The most critical aspect to be considered when creating the database is certainly the definition of the number of scenarios to be simulated. The goal is to achieve a good balance between the manageability of the database and its representativeness of different inundation patterns that may occur in the area, both in terms of breach location and of hydrological conditions. Bearing in mind that a real event will never exactly match any hypothetical scenario, a discrete well-thought-out number of simulations will still provide inundation predictions that are accurate enough from a practical point of view.

A suitable distance between hypothetical breaches must be defined first. A spacing in the order of 1-10 km can be considered adequate, depending on the river characteristics. For example, in the present work, a relatively dense spacing (around 2-3 km) was selected for the Panaro River (cross-sectional width ~100-200 m; upstream basin ~1000 km^2; flood discharge ~100-1000 m^3/s). For a larger river (e.g. Po River, cross-sectional width ~1000 m; upstream basin ~70'000 km^2; flood

625 discharge ~10'000 m^3/s), for which the breach outflow volume can be expected to be even two
626 orders of magnitude larger, a coarser spacing (up to 10 km) can be considered acceptable to
627 obtain a reliable inundation prediction. As a rule of thumb, the ratio of spacing to cross-sectional
628 width can be assumed around 10-20. However, the breach locations must not necessarily be
629 equally spaced, as other considerations should guide the selection of their location, such as the
630 knowledge of "fragile" levee sections and the topography. For example, the presence of embanked
631 roads/railways or other topographical discontinuities close to the levee can strongly influence the
632 flood dynamics and constrain the choice of the breach locations, which should be placed both
633 upstream and downstream of these discontinuities (Ferrari et al., 2020). Following these criteria in
634 the selection of breach locations, flooding due to failures at intermediate locations can be expected
635 to differ from the closest hypothetical scenario only near the breach sites. Actually, this is the area
636 that benefits the least from early warning in any case, because it is flooded immediately after the
637 breach triggering, well before any emergency activity can be put in place. Therefore, from a
638 practical point of view, the possible inaccuracy related to the breach location can be partially
639 neglected as regards the inundation extent, while it should be kept in mind as regards the flood
640 arrival times, as discussed before.
641 As regards the hydrological conditions, two inflow hydrographs must be selected at least,
642 corresponding to events during which two different types of breach triggering mechanisms can take
643 place (overtopping and non-overtopping). While the former occurs only for medium-low probability
644 events (depending on the design return period of the levee system), the latter can occur even for
645 more frequent events due to piping or internal erosion induced by dens of burrowing animals, etc.,
646 as recent events indicated (Orlandini et al., 2015). Additional inflow conditions can be considered
647 when creating the database, but multiplying the number of hydrological scenarios does not actually
648 ease the identification of the one closest to the current event during real-time emergency
649 management, since real-time estimates of discharge are highly uncertain and the return period of
650 the event can only be determined ex-post. A simple dichotomy (overtopping or non-overtopping)
651 can somehow facilitate the selection of the corresponding scenario (Inflow A or B) during
652 emergencies. Moreover, although water levels and flood arrival times can be characterized by

larger uncertainties in case of large differences in inflow conditions, the identification of the inundated area can still be obtained from the available pre-simulated scenarios, as already discussed in Section 4.1. In fact, on the one hand, topography plays a key role in the inundation propagation; on the other hand, the most critical factor to obtain reliable flood maps is the correct estimation of the breach outflow volume, rather than the inflow hydrograph in the river. Interestingly, the results presented in this work even show that the breach outflow volume does not necessarily increase with the hydrograph's volume, since other factors may influence the latter (e.g. shape of flood hydrograph, breach evolution). Therefore, the inflow conditions in the database need to be representative of different typical flood events in the river, so that realistic breach outflow volumes can be obtained in pre-simulated scenarios. To this end, the SDHs obtained from the method proposed by Tomirotti & Mignosa (2017), used in this work, have the advantage that not only the peak discharge, but also the flood volume and time distribution (i.e. the hydrograph's shape) derive from statistical considerations on historical discharges. Finally, it is worth clarifying that the hydrographs must not necessarily correspond to a pre-defined return period, though this is recommended in the practice for integration with flood hazard assessments.

In addition to the already discussed drawback of the possible uncertainties in the prediction of flood arrival times, another limitation of the proposed strategy is the fact that simulations in the database neglect all emergency interventions, which are difficult to identify a priori. Indeed, even if the current conditions during a real event exactly matched the assumptions made for the hypothetical scenario, the actual inundation could still deviate from the pre-simulated results in the very likely case that flood mitigation measures were undertaken (e.g. flood barriers, dewatering pumps or relief cuts in embankments of minor channels for drainage purposes, breach closure operations). The pre-simulated scenarios cannot be modified "on the fly" during the event to consider these interventions, and therefore may provide a somewhat conservative prediction that overestimates the impact of the inundation, possibly leading to false alarms in some areas. However, this issue is also present for real-time simulations. Finally, it is worth mentioning that the strategy would provide inaccurate inundation predictions in "extreme" or particular cases, such as if a very severe flood event generated extensive levee overtopping and breaching at multiple locations along the river, or

if a concurrent breach opened on the levee of a nearby watercourse inducing an overlapping inundation in the same area.

5. CONCLUSIONS

In this work, the real test case of the inundation caused by a levee breach on the Panaro River, occurred in December 2020, was used to assess the effectiveness of the strategy of creating an off-line database of pre-simulated scenarios for civil protection purposes (Ferrari et al., 2020). The results and discussion suggest that the development of such database for lowland areas can be a useful “surrogate” tool for the prediction of the possible inundations induced by a river levee breach. This methodology can be viewed as a non-structural measure useful for early warning and for decision making concerning emergency activities, and can be potentially applied to other areas at risk of flooding in case of levee collapse.

ACKNOWLEDGEMENTS

The Authors would like to thank the Municipality of Nonantola (Modena, Italy), Arch. Carla Ferrari and her collaborators for providing field data. This research benefits from the HPC facility of the University of Parma. The support of CINECA under project NEMORINO (ID: HP10CR41J6) is also gratefully acknowledged. The anonymous Reviewers also provided valuable suggestions that contributed to improving the quality of the manuscript.

APPENDIX A. Comparison of different hypothetical scenarios

Figure A1 shows an example of the flooded areas obtained from pre-simulated scenarios in the database, characterized by different breach locations and inflow conditions.

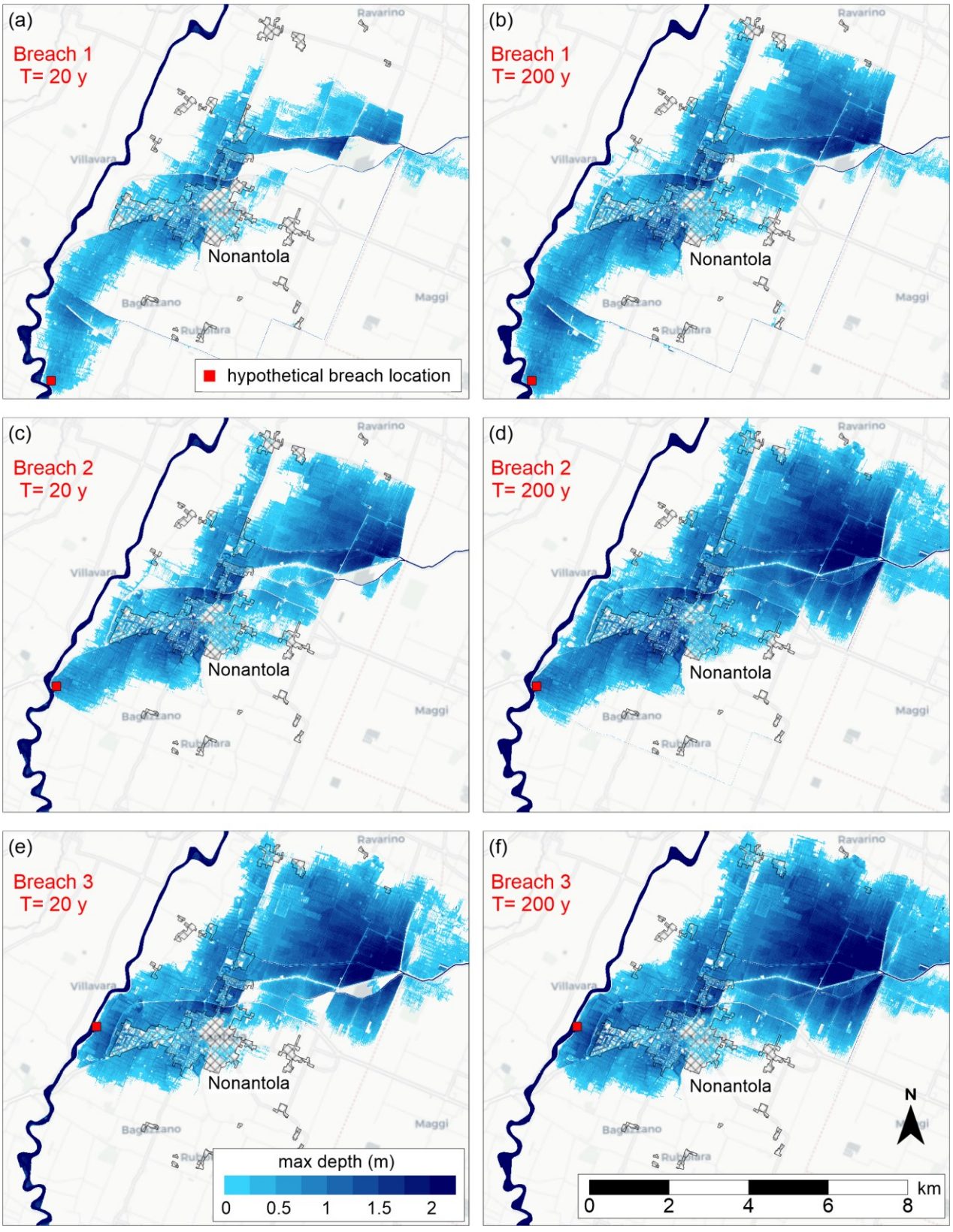

Figure A1. Comparison of the maximum water depths for different hypothetical scenarios in the database (T = 20 years on the left panels, T = 200 years on the right panels; Breaches 1, 2, and 3 from top to bottom).

REFERENCES

Arrighi, C., Pregnolato, M., Dawson, R. J., & Castelli, F. (2019). Preparedness against mobility disruption by floods. Science of the Total Environment, 654, 1010-1022.

Bachmann, D., Eilander, D., De Leeuw, A., De Bruijn, K., Diermanse, F., Weerts, A., & Beckers, J. (2016). Prototypes of risk-based flood forecasting systems in the Netherlands and Italy. In E3s web of conferences (Vol. 7, p. 18018). EDP Sciences.

Bhola, P. K., Leandro, J., & Disse, M. (2018). Framework for offline flood inundation forecasts for two-dimensional hydrodynamic models. Geosciences, 8(9), 346.

Bihan, G. L., Payrastre, O., Gaume, E., Moncoulon, D., & Pons, F. (2017). The challenge of forecasting impacts of flash floods: test of a simplified hydraulic approach and validation based on insurance claim data. Hydrology and Earth System Sciences, 21(11), 5911-5928.

Dazzi, S., Shustikova, I., Domeneghetti, A., Castellarin, A., & Vacondio, R. (2021). Comparison of two modelling strategies for 2D large-scale flood simulations. Environmental Modelling & Software, 105225.

Dazzi, S., Vacondio, R., & Mignosa, P. (2019). Integration of a levee breach erosion model in a GPU-accelerated 2D shallow water equations code. Water Resources Research, 55(1), 682-702.

Di Baldassarre, G., Kreibich, H., Vorogushyn, S., Aerts, J., Arnbjerg-Nielsen, K., Barendrecht, M., ... & Ward, P. J. (2018). Hess Opinions: An interdisciplinary research agenda to explore the unintended consequences of structural flood protection. Hydrology and Earth System Sciences, 22(11), 5629-5637.

Dottori, F., Di Baldassarre, G., & Todini, E. (2013). Detailed data is welcome, but with a pinch of salt: Accuracy, precision, and uncertainty in flood inundation modeling. Water Resources Research, 49, 6079-6085.

Dottori, F., Kalas, M., Salamon, P., Bianchi, A., Alfieri, L., & Feyen, L. (2017). An operational procedure for rapid flood risk assessment in Europe. Natural Hazards and Earth System Sciences, 17(7), 1111-1126.

734 Ferrari, A., Dazzi, S., Vacondio, R., & Mignosa, P. (2020). Enhancing the resilience to flooding
735 induced by levee breaches in lowland areas: a methodology based on numerical modelling.
736 Natural Hazards and Earth System Sciences, 20(1), 59-72.
737 Govi, M., & Maraga, F. (2005). Inundation on the Po Plain caused by levee breaches, Giornale di
738 Geologia Applicata, 1, 167–176.
739 Huthoff, F., Remo, J. W., & Pinter, N. (2015). Improving flood preparedness using hydrodynamic
740 levee-breach and inundation modelling: Middle Mississippi River, USA. Journal of Flood Risk
741 Management, 8(1), 2-18.
742 Jongman, B. (2018). Effective adaptation to rising flood risk. Nature communications, 9(1), 1-3.
743 Krzhizhanovskaya, V. V., Shirshov, G. S., Melnikova, N. B., Belleman, R. G., Rusadi, F. I.,
744 Broekhuijsen, B. J., ... & Meijer, R. J. (2011). Flood early warning system: design, implementation
745 and computational modules. Procedia Computer Science, 4, 106-115.
746 Kron, A., Nestmann, F., Schlüter, I., Schädler, G., Kottmeier, C., Helms, M., ... & Krejčí, J. (2010).
747 Operational flood management under large-scale extreme conditions, using the example of the
748 Middle Elbe. Natural Hazards and Earth System Sciences, 10(6), 1171-1181.
749 Liu, Z., Merwade, V., & Jafarzadegan, K. (2019). Investigating the role of model structure and
750 surface roughness in generating flood inundation extents using one-and two-dimensional hydraulic
751 models. Journal of Flood Risk Management, 12(1), e12347.
752 Ludy, J., & Kondolf, G. M. (2012). Flood risk perception in lands “protected” by 100-year levees.
753 Natural hazards, 61(2), 829-842.
754 Manselli, L., Molinari, D., Pogliani, A., Zambrini, F., & Menduni, G. (2022). Improvements and
755 Operational Application of a Zero-Order Quick Assessment Model for Flood Damage: A Case
756 Study in Italy. Water, 14(3), 373.
757 Masseroni, D., Cislaghi, A., Camici, S., Massari, C., & Brocca, L. (2017). A reliable rainfall–runoff
758 model for flood forecasting: review and application to a semi-urbanized watershed at high flood risk
759 in Italy. Hydrology Research, 48(3), 726-740.
760 Menduni, G., Cocchi, R., Manselli, L., & Simonini, P. (2021). Commissione tecnico-scientifica per la
761 valutazione delle cause all'origine della rotta arginale lungo il fiume Panaro in località Gaggio di

762 Castelfranco Emilia – Relazione di dettaglio. Regione Emilia-Romagna, Bologna (Technical-
763 scientific committee for evaluating the causes of the levee collapse on the Panaro River near
764 Gaggio di Castelfranco Emilia – Detailed report: Emilia-Romagna Region, Bologna, in Italian).
765 Merz, B., Kuhlicke, C., Kunz, M., Pittore, M., Babeyko, A., Bresch, D. N., ... & Wurpts, A. (2020).
766 Impact forecasting to support emergency management of natural hazards. Reviews of geophysics,
767 58(4), e2020RG000704.
768 Ming, X., Liang, Q., Xia, X., Li, D., & Fowler, H. J. (2020). Real-time flood forecasting based on a
769 high-performance 2-D hydrodynamic model and numerical weather predictions. Water Resources
770 Research, 56(7), e2019WR025583.
771 Mosavi, A., Ozturk, P., & Chau, K. W. (2018). Flood prediction using machine learning models:
772 Literature review. Water, 10(11), 1536.
773 Mourato, S., Fernandez, P., Marques, F., Rocha, A., & Pereira, L. (2021). An interactive Web-GIS
774 fluvial flood forecast and alert system in operation in Portugal. International Journal of Disaster
775 Risk Reduction, 58, 102201.
776 Nguyen, P., Thorstensen, A., Sorooshian, S., Hsu, K., & AghaKouchak, A. (2015). Flood
777 forecasting and inundation mapping using HiResFlood-UCI and near-real-time satellite
778 precipitation data: The 2008 Iowa flood. Journal of Hydrometeorology, 16(3), 1171-1183.
779 Oliver, J., Qin, X. S., Larsen, O., Meadows, M., & Fielding, M. (2018). Probabilistic flood risk
780 analysis considering morphological dynamics and dike failure. Natural hazards, 91(1), 287-307.
781 Orlandini, S., Moretti, G., & Albertson, J. D. (2015). Evidence of an emerging levee failure
782 mechanism causing disastrous floods in Italy. Water Resources Research, 51(10), 7995-8011.
783 Pappenberger, F., Cloke, H. L., Parker, D. J., Wetterhall, F., Richardson, D. S., & Thielen, J.
784 (2015). The monetary benefit of early flood warnings in Europe. Environmental Science & Policy,
785 51, 278-291.
786 Plate, E. J. (2002). Flood risk and flood management. Journal of hydrology, 267(1-2), 2-11.
787 Rai, R. K., van den Homberg, M. J., Ghimire, G. P., & McQuistan, C. (2020). Cost-benefit analysis
788 of flood early warning system in the Karnali River Basin of Nepal. International journal of disaster
789 risk reduction, 47, 101534.

790 Ritter, J., Berenguer, M., Corral, C., Park, S., & Sempere-Torres, D. (2020). ReAFFIRM: real-time
791 assessment of flash flood impacts–a regional high-resolution method. Environment international,
792 136, 105375.
793 Salvati, P., Bianchi, C., Rossi, M., & Guzzetti, F. (2010). Societal landslide and flood risk in Italy.
794 Natural Hazards and Earth System Sciences, 10(3), 465-483.
795 Schubert, J. E., & Sanders, B. F. (2012). Building treatments for urban flood inundation models and
796 implications for predictive skill and modeling efficiency. Advances in Water Resources, 41, 49-64.
797 https://doi.org/10.1016/j.advwatres.2012.02.012
798 Tadesse, Y. B., & Fröhle, P. (2020). Modelling of Flood Inundation due to Levee Breaches:
799 Sensitivity of Flood Inundation against Breach Process Parameters. Water, 12(12), 3566.
800 Tarrant, O., Todd, M., Ramsbottom, D., & Wicks, J. (2005). 2D floodplain modelling in the tidal
801 Thames – Addressing the residual risk. Water and Environment Journal, 19(2), 125-134.
802 Tomirotti, M., & Mignosa, P. (2017). A methodology to derive Synthetic Design Hydrographs for
803 river flood management. Journal of Hydrology, 555, 736-743.
804 Vacondio, R., Dal Palù, A., & Mignosa, P. (2014). GPU-enhanced finite volume shallow water
805 solver for fast flood simulations. Environmental Modelling & Software, 57, 60-75.
806 Vacondio, R., Aureli, F., Ferrari, A., Mignosa, P., & Dal Palù, A. (2016). Simulation of the January
807 2014 flood on the Secchia River using a fast and high-resolution 2D parallel shallow-water
808 numerical scheme. Natural Hazards, 80(1), 103-125.
809 Vacondio, R., Dal Palù, A., Ferrari, A., Mignosa, P., Aureli, F., & Dazzi, S. (2017). A non-uniform
810 efficient grid type for GPU-parallel Shallow Water Equations models. Environmental Modelling &
811 Software, 88, 119-137.
812 Viero, D. P., D'Alpaos, A., Carniello, L., & Defina, A. (2013). Mathematical modeling of flooding due
813 to river bank failure. Advances in Water Resources, 59, 82-94.
814 Visser, P. J. (1999). Breach erosion in sand-dikes. In Coastal Engineering 1998, 3516-3528.
815 Vorogushyn, S., Merz, B., Lindenschmidt, K. E., & Apel, H. (2010). A new methodology for flood
816 hazard assessment considering dike breaches. Water resources research, 46(8).

817 Yu, D., & Lane, S. N. (2006). Urban fluvial flood modelling using a two-dimensional diffusion-wave
818 treatment, part 1: mesh resolution effects. Hydrological Processes: An International Journal, 20(7),
819 1541-1565.
820 Zhang, W., Zhou, J., Liu, Y., Chen, X., & Wang, C. (2016). Emergency evacuation planning against
821 dike-break flood: a GIS-based DSS for flood detention basin of Jingjiang in central China. Natural
822 Hazards, 81(2), 1283-1301.